CONF-9508143--1

SAND95-1602C

Beneficial Effects of the Aluminum Alloy Process as Practiced in the Photovoltaic Device Fabrication Laboratory

W. Kent Schubert
Photovoltaic Systems Components Department
Sandia National Laboratories

ABSTRACT - The aluminum alloy process implemented in Sandia's Photovoltaic Device Fabrication Laboratory (PDFL) has major beneficial effects on the performance of commercial multicrystalline-silicon (mc-Si) substrates. Careful analysis of identically processed cells (except for the alloyed layer) in matched mc-Si substrates clearly indicates that the majority of the benefit arises from improved bulk minority carrier diffusion length. Based on spectral response measurements and PC-1D modeling we have observed improvements due to the alloy process of up to 400% in the "average" diffusion length in moderate-area cells and around 50% in large-area cells. The diffusion length is dramatically improved in the interior of the silicon grains in alloyed substrates, resulting in the majority of the recombination occurring at the grain boundaries and localized areas with high defect densities.

1.0 The Challenge

The challenge for all solar cell technologies is to lower the cost per watt. One approach is to improve the conversion efficiency without disproportionately raising the cost. High-efficiency enhancements are only useful if they can be implemented cost-effectively. A informative review of several efficiency enhancement techniques and their costs for mc-Si cell processing is found in [1]. One of the potentially viable techniques identified in that review is the aluminum-alloy back-surface-field process. Several groups have investigated the beneficial effects of this process and some of the best cell results using the process are reported in [2-5]. The aluminum-alloy back-surface-field process can improve cell efficiency both through gettering of fast-diffusing impurities [6] and reflection of carriers from the back contact. The latter mechanism is important only if the minority carrier diffusion length (L) is comparable to, or larger than the cell thickness (W). For most mc-Si cells to date the benefit of the alloy process must come primarily from the gettering effects, since L/W is typically less than unity.

This paper reports on our experience in Sandia's Photovoltaic Device Fabrication Laboratory (PDFL) using the aluminum-alloy process on mc-Si cells. In the past we have reported the results of a statistically designed gettering study on several commercial mc-Si materials which included both phosphorus diffusions and aluminum-alloy treatments [7]. The present work looks more carefully at the effects of the aluminum alloy treatment alone on just one of those materials (cast mc-Si material manufactured by Solarex Corporation). In [7] we were unable to identify an optimal combination of times and temperatures for the phosphorus and aluminum treatments for this material. In addition, we observed no interactions between the two processes for Solarex material. However, the previous study did not include omitting the aluminum-alloy treatment completely (alloying temperatures from 700 to 900°C were used, all of which are above the Al-Si eutectic temperature). In this study we compare the

This work was performed by Sandia National Laboratories for the US Department of Energy under contract DE-AC04-94AL85000.

performance of both moderate- and large-area cells produced with and without the aluminum-alloy treatment in substrates with matched grain structures.

2.0 Materials and Methods

2.1 Cell Processing

The mc-Si cell process used in the PDFL has been discussed in detail elsewhere [5]. The process is summarized in Table 1. This process produces passivated emitter cells with evaporated, photolithographically defined grids, and a double-layer antireflection (DLAR) coating of TiO_2/Al_2O_3.

Results of two experiments will be discussed in this paper, both using 1-Ωcm mc-Si produced by Solarex. In both experiments, substrates with matched grain structures (vertical near neighbors from the same ingot) were used to minimize differences in as-grown material quality. In the first experiment, nine-cell arrays of 4.65-cm^2 cells were produced in collaboration with Solarex to compare two backside processing sequences. Half the cells in this experiment went through the complete PDFL process as outlined in Table 1. The second half of the cells skipped the aluminum deposition steps for the alloy process and the back contact but did go through all of the furnace steps. PDFL processing was stopped after the forming gas anneal, and processing was then completed at Solarex with their conventional non-alloyed aluminum back contact and the deposition of a single-layer antireflection (SLAR) coating of TiO_2. Therefore, the two splits differed in the back surface treatment (alloyed vs. non-alloyed aluminum) and the antireflection coating (Sandia's DLAR vs Solarex's SLAR). The second experiment was similar, except that all processing was done in the PDFL and large-area (42 cm^2) cells were used. In this second experiment, the only processing difference was that half the cells did not get the aluminum deposition for the alloy formation.

2.2 Cell Characterization

One-sun measurements were done to characterize all cells, and matched cells were selected for more thorough testing, including dark current-voltage (I-V), spectral hemispherical reflectance, absolute spectral response, and laser-beam-induced current (LBIC) mapping. A two-diode model was used to fit the one-sun and dark I-V curves. The model incorporates four fitting parameters (series resistance R_s, shunt resistance R_{sh}, n = 1 saturation current I_{01}, and n = 2 saturation current I_{02} where n is the diode ideality factor) to obtain a reasonable fit to the I-V curves, particularly in the region around the maximum power voltage. Mijnarends, *et al* [8] have pointed out that in materials with laterally nonuniform spectral response, the distribution of diffusion lengths (in addition to nonideal recombination) affects the magnitude of I_{02} determined from such a model. The absolute spectral response and reflectance were used to calculate the external and internal quantum efficiency (EQE and IQE respectively). Extended analysis of the IQE was used to determine the minority carrier diffusion length (L), back surface reflectance, and where possible, the back surface recombination velocity (S_b). Parameters determined from the above analyses were used in PC-1D to model the cells. Laser-beam-induced current mapping was done at 1060 nm to generate carriers throughout

the entire thickness of the cells. Comparison of LBIC maps for matched cells gives a qualitative indication of the magnitude and uniformity of the gettering effects.

3.0 Results and Discussion

Table 2 summarizes the results of the first experiment using moderate-area cells. The currents and efficiencies of the cells with the Solarex SLAR have been adjusted upward to account for the higher solar-weighted front-surface reflectance in comparison with the Sandia DLAR. The major differences in performance occur in the short-circuit current and open-circuit voltage.

Matched cells (with respect to grain structure) with both types of back surface treatment, and with closely matched fill factors, were chosen for further characterization and analysis. Two-diode modeling indicated that the series and shunt resistance values for the two cells were very similar and inflicted no performance penalty. Furthermore, the $n = 1$ and $n = 2$ saturation current densities (I_{01} and I_{02}) were such that the performance limitation due to $n = 2$ recombination was essentially the same in both cells (25 to 30% of the total recombination losses at the maximum power point).

Analysis of the absolute spectral response measured in a small area (approximately 5-mm X 5-mm) near the center of each cell indicated that the minority carrier diffusion length (L) increased from about 70 μm in the cell with the aluminum-sprayed back contact, to about 180 μm in the cell receiving the aluminum alloy treatment. LBIC maps for the two cells are shown in the upper panels of Fig.1. Clearly the alloy treatment has improved the carrier lifetime in most of the grain interiors, leaving the grain boundaries and a few small grains as the most prominent recombination features. Histograms of the LBIC response (see the lower panels of Fig. 1) provide a good description of the distribution of diffusion lengths. The LBIC histogram of the unalloyed cell has a nearly symmetric response peak, while the LBIC histogram of the alloyed cell has a sharply asymmetric response peak with the bulk of the response pushed toward higher currents. The shape of these histograms could be used to determine the distribution of diffusion lengths used in the two-diode model of [8].

Measured or calculated values were used wherever possible to model the cells of Fig. 1 using PC-1D. Slightly improved agreement with the measured performance was achieved by assuming $L = 50$ μm (rather than the 70 μm determined at the center) for the non-alloyed cell and 220 μm (rather than 180 μm) for the alloyed cell. This implies that the "average" diffusion length was improved by about a factor of four by the alloy treatment.

Table 3 shows the one-sun performance for large-area (42-cm^2) cells produced in the second experiment using a different batch of Solarex mc-Si material. Although the difference is not as large as with the smaller cells discussed above, the performance of the alloyed large-area cells is significantly better than that of the sintered cells. The LBIC maps for two cells (Fig. 2) again show that the alloy treatment has cleaned up the majority of the grain interiors, leaving the grain boundaries and scattered small "ungettered" areas as the performance inhibitors. As

expected, the LBIC histograms in the lower panels of Fig. 2 show the same shift of the weight of the response distribution to higher currents in the alloyed cell. Two-diode modeling of the two types of cells again showed no difference in the relative amount of non-ideal recombination between the alloyed and sintered cells.

4.0 Conclusions

It is clear from the present results that the aluminum alloy treatment effectively getters mc-Si substrates. This is in agreement with prior studies in other laboratories. Although the present study does not attempt to eliminate interactions with the emitter diffusion treatment, it appears from our experience that the preponderance of the gettering occurs during the subsequent aluminum alloy anneal. The aluminum alloy treatment used here does not eliminate all high-recombination areas in the Solarex mc-Si. Localized regions with (apparently) high dislocation densities are not significantly improved and become the dominant recombination centers in the alloyed cells.

References

[1] S. Narayanan and J. Wohlgemuth, Prog. in Photovoltaics: Research and Applications, 2 (1994) 121.

[2] S. Narayanan, S. R. Wenham, and M. A. Green, IEEE Trans. Electron Devices ED-37 (1990) 382.

[3] P. Sana, J. Salami, and A. Rohatgi, IEEE Trans. Electron Devices ED-40 (1993) 1461.

[4] H. Nakaya, M. Nishida, Y. Takeda, S. Moriuchi, T. Tonegawa, T. Machida, and T. Nunoi, Tech. Digest of the International PVSEC-7, Nagoya, Japan (1993) 91.

[5] W. K. Schubert, D. L. King, T. D. Hund, and J. M. Gee, Solar Energy Materials and Solar Cells (to be published).

[6] S. M. Joshi, U. M. Gosele, and T. Y. Tan, J. Appl. Phys. 77 (1995) 3858.

[7] W. K. Schubert, IEEE 1st World Conf. on Photovoltaic Energy Conversion, Waikoloa, HI (1994) 1595.

[8] P. E. Mijnarends, G. J. M. Janssen, and W. C. Sinke, 11th E. C. Photovoltaic Solar Energy Conf., Montreux, Switzerland (1992) 310.

Table 1. PDFL High-Efficiency Single-Photomask Process for mc-Si Solar Cells

Moderate-Area	Both	Large-Area
	70°C KOH, or HNO_3/HF damage removal etch	
	HCl clean	
	APCVD-oxide - Back, 400°C (optional)	
	$POCl_3$ One-step emitter diffusion/drive-in (80-100Ω/□, 875°C)	
APCVD-oxide - Front, 400°C		
Laser scribe isolation grooves		
KOH groove etch		
	Deglaze front and back	
	HCl clean	
	Aluminum deposition (back, 1 μm)	
	Aluminum-alloy anneal, ≤ 900°C (also grows passivation oxide on front)	
	Photolithographic definition of front grid	
	Contact oxide etch	
	TiPdAg deposition (front)	
	Al deposition (back, plus TiPdAg if cell will be soldered)	
	Lift-off	
	Forming gas anneal/Metal Sintering (400°C)	
		Ag electroplating
	TiO_2/Al_2O_3 DLAR deposition	
		Separation laser scribe and cleave (back)

Table 2. Wafer-average performance summary for 4.65-cm^2 cells with either an aluminum-alloyed back surface treatment (wafers 1 and 5) or an unalloyed aluminum back surface treatment (wafers 2 and 6).

Wafer	Back Surface Treatment	V_{oc} (volts)	V_{oc} s.d. (volts)	J_{sc} (mA/cm^2)	J_{sc} s.d. (mA/cm^2)	Fill Factor	Fill Factor s.d.	Eff. (%)	Eff. s.d. (%)
1	PDFL Al-Alloy	0.611	0.003	33.5	0.2	0.792	0.004	16.3	0.3
5	PDFL Al-Alloy	0.610	0.003	33.5	0.2	0.790	0.015	16.2	0.4
2	Solarex Al-Spray	0.574	0.002	29.9*	0.4	0.772	0.014	13.2*	0.2
6	Solarex Al-Spray	0.581	0.003	31.4*	0.6	0.767	0.027	13.9*	0.4

* These entries were adjusted upward to account for the difference in solar-weighted reflectance between Sandia's DLAR (6.6%) and Solarex's SLAR (15.6%).

Table 3. One-sun performance for large-area cells without and with the aluminum alloy treatment.

Cell Name	Back Surface Treatment	V_{oc} (volts)	J_{sc} (mA/cm^2)	Fill Factor	Eff. (%)
SOL-4/W 2	sintered	0.593	30.0	0.759	13.5
SOL-4/W 3	sintered	0.594	30.1	0.765	13.7
SOL-4/W 4	sintered	0.595	30.1	0.772	13.8
SOL-4/W 5	sintered	0.594	30.0	0.773	13.8
SOL-4/W 6	sintered	0.594	30.0	0.768	13.7
Avg.	*sintered*	*0.594*	*30.0*	*0.767*	*13.7*
s.d.	*sintered*	*0.001*	*0.04*	*0.005*	*0.10*
SOL-4/W 8	alloyed	0.604	31.8	0.764	14.7
SOL-4/W 9	alloyed	0.605	31.6	0.771	14.8
SOL-4/W 11	alloyed	0.605	31.7	0.771	14.8
SOL-4/W 12	alloyed	0.604	31.7	0.771	14.8
SOL-4/W 13	alloyed	0.605	31.6	0.770	14.8
Avg.	*alloyed*	*0.605*	*31.7*	*0.770*	*14.8*
s.d.	*alloyed*	*0.0004*	*0.06*	*0.003*	*0.04*

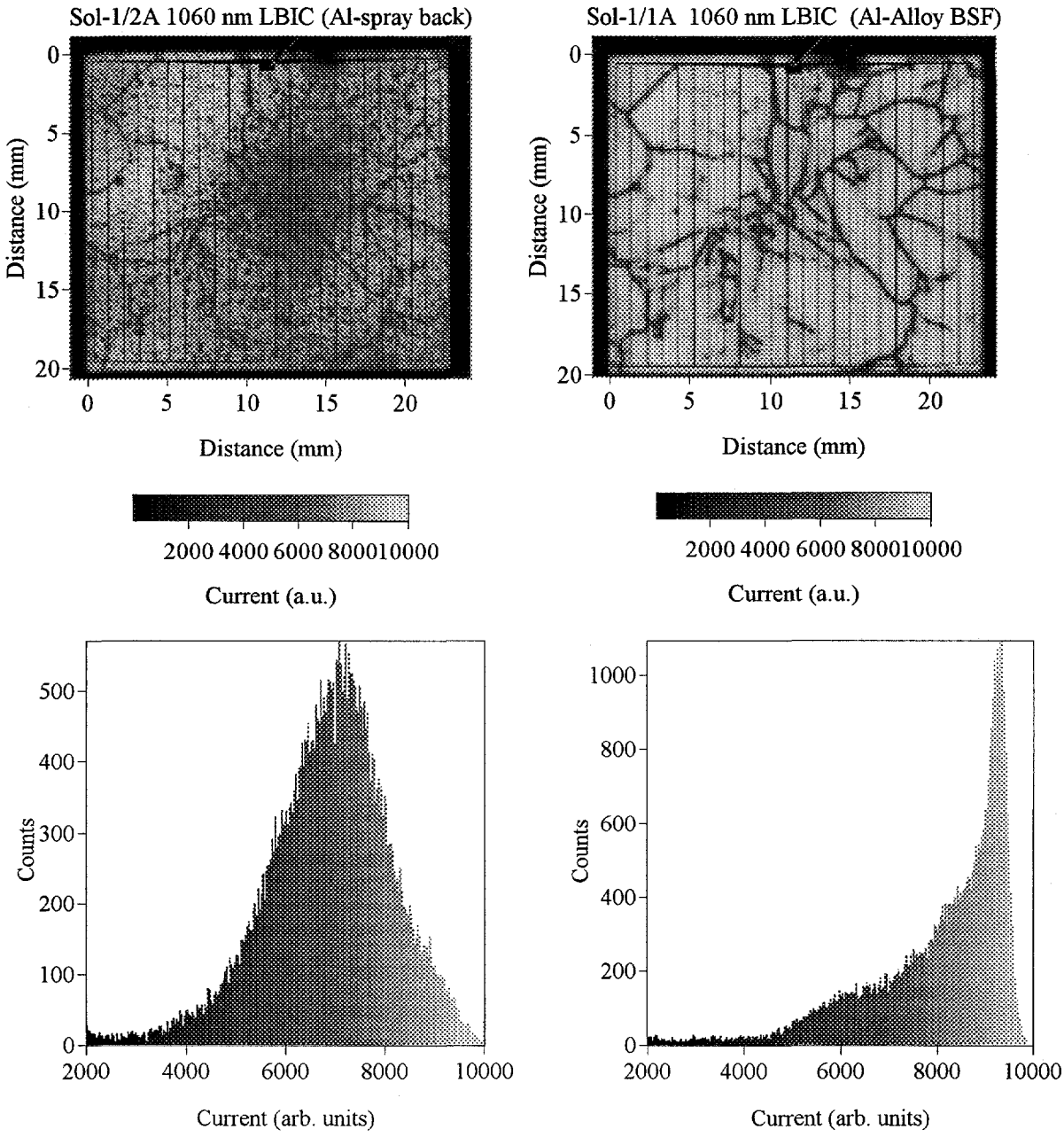

Fig. 1. The upper panels show laser-beam-induced current (LBIC) maps taken at 1060 nm of moderate-area mc-Si solar cells with matched grain structures. The map on the left is of a cell with a non-alloyed aluminum back contact. The map on the right is of a cell with an aluminum-alloyed back contact. The alloy process has clearly eliminated much of the recombination occurring in the grain interiors. The histograms in the lower panels illustrate how the alloy process has affected the distribution of localized diffusion lengths (note the difference in vertical scales).

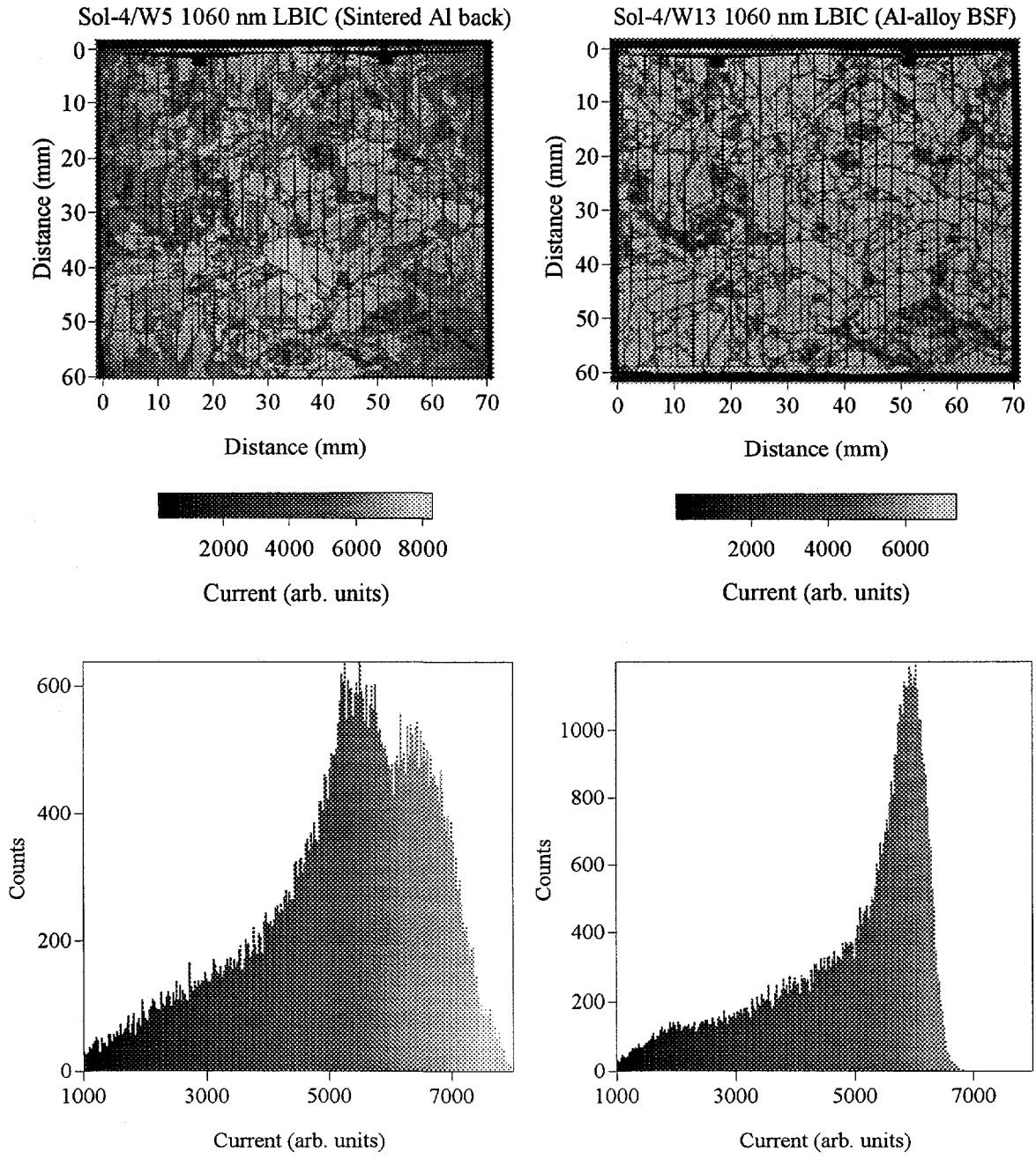

Fig. 2. LBIC maps of large-area cells again illustrating how the alloy process has reduced carrier recombination in most of the grain interiors. Remaining regions of high recombination are still apparent even in the alloyed cell (right-hand panel). The histograms in the lower panels qualitatively illustrate the shift of the distribution of localized diffusion lengths to longer values. Note the different vertical scales for the histograms, and that the current scales are not directly related.